Article

The Plagiochilins from *Plagiochila* Liverworts: Binding to α-Tubulin and Drug Design Perspectives

Gérard Vergoten [1] and Christian Bailly [2,3,*]

1   Inserm, U1286—INFINITE—Lille Inflammation Research International Center, ICPAL, University Lille, 3 Rue du Professeur Laguesse, 59000 Lille, France
2   CNRS, Inserm, CHU Lille, UMR9020-U1277—CANTHER—Cancer Heterogeneity Plasticity and Resistance to Therapies, University of Lille, 59000 Lille, France
3   Oncowitan, Scientific Consulting Office, Wasquehal, 59290 Lille, France
*   Correspondence: christian.bailly@univ-lille.fr

Abstract: Among bryophytes, the *Plagiochila* genus represents a large group of leafy liverworts with over 500 species. Plagiochilins A to X are sesquiterpenoids isolated from Plagiochila species. The lead compound plagiochilin A (Plg-A), endowed with anticancer and antiparasitic properties, has been characterized as a potent mitosis inhibitor, acting selectively at the late stage of cytokinesis termed abscission. The compound perturbs the dynamics of microtubules, blocking cell cycle progression and triggering the death of malignant cells. Based on the compound's mechanism of action and by analogy with other natural products bearing a dihydro-pyrone moiety, we postulated that Plg-A could bind to the pironetin site of α-tubulin. A molecular docking analysis was performed to compare the bindings of all 24 plagiochilins to α-tubulin and to establish structure–binding relationships. The identification of Plg-E and Plg-G as the best binders in the series highlighted the importance of the C13-OH or C=O group for α-tubulin recognition. This observation led to the testing of the natural-product ester plagiochilin A-15-yl n-octanoate and the corresponding alcohol (Plg-OH), both identified as robust α-tubulin binders. The study provides a rationale to potentially explain the mechanism of action of Plg-A and to guide the design of new derivatives.

Keywords: anticancer agents; microtubules; molecular docking; *Plagiochila* species; plagiochilin A; α-tubulin

1. Introduction

Bryophytes were among the first photosynthetic organisms to colonize the terrestrial environment. The group includes mosses, hornworts and liverworts, which are found in nearly all terrestrial habitats on all continents [1]. The medicinal use of bryophytes dates to ancient times, with the first testimonies reported in the 16th century [2]. A wide diversity of chemical compounds can be isolated from bryophytes (notably liverworts), including many terpenoids of prime pharmacological interest [3,4]. A wide diversity of sesqui- and diterpenoids have been isolated and their antimicrobial, antifungal, cytotoxic, anti-inflammatory and antiparasitic activities characterized [5]. We were particularly interested in bioactive natural products isolated from liverworts of the genus *Plagiochila*.

Plagiochilin A (hereafter designated Plg-A) (Figure 1) is a secoaromadendrane-type sesquiterpenoid first isolated 45 years ago from the liverworts *Plagiochila yokogurensis* Steph. and *Plagiochila hattoriana* Inoue [6,7]. Later, the product was found in other *Plagiochila* species, such as *P. semidecurrens*, *P. pulcherrima* Horik. and *P. disticha* (Lehm. & Lindenb.) Lindenb. [8–10]. Plagiochilin A was initially characterized as a strong insect antifeedant agent, but this natural product displays a range of bioactivities, including insecticidal, anti-inflammatory, antiparasitic and antiproliferative properties. Notably, the compound has been shown to reduce the growth of P-388 leukemia cells with good efficacy ($IC_{50} = 3.0 \ \mu g/mL$) [11]. Another study demonstrated that Plg-A can inhibit the growth of

a range of tumor cell lines, including prostate, breast, lung and leukemia cells [10]. The compound proved particularly efficient at inhibiting the growth of DU145 prostate cancer cells, with an efficacy superior to the reference anticancer drug fludarabine phosphate (GI_{50} = 3.0 µM) [10].
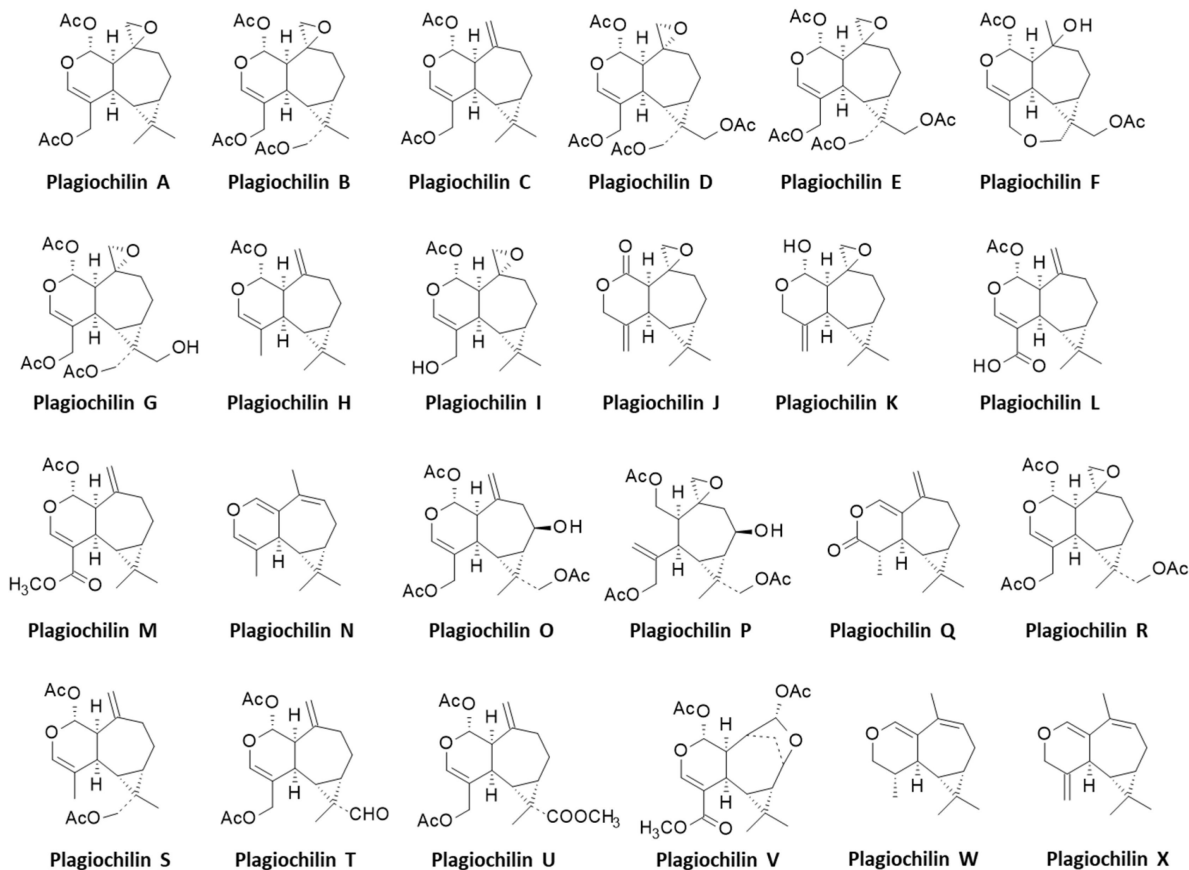

Figure 1. Structures of plagiochilins.

Plagiochilin A is the leading member of a series of 24 derivatives, designated plagiochilins A to X (Figure 1), discovered over the past 40 years. Plagiochilins are all natural products isolated from diverse *Plagiochila* species between 1978 (Plg-A) and 2005 (Plg-X), as reviewed recently [12]. They are seco-aromadendrane-type sesquiterpenoids considered as chemosystematic markers in the Plagiochilaceae [13]. The pharmacological properties of plagiochilins A and C have been investigated, but the other compounds have rarely been studied [12]. A recent work identified a key aspect of the mechanism of action of Plg-A. The compound was shown to block DU145 cell division by preventing completion of cytokinesis, stopping cell cycle progression at the G2/M phase. Plg-A induced a blockade of cell division at the membrane abscission stage, which is the late stage of cytokinesis, thereby triggering cell apoptosis (Figure 2). The process is characterized by cytoskeletal effects involving the rearrangement of microtubules and implicating α-tubulin [14]. Cytokinetic abscission is a well-orchestrated, tightly regulated process that influences cell fate and tissue growth [15]. It involves different proteins containing microtubule-interacting and trafficking (MIT) domains. A microtubule-rich structure formed during cytokinesis called the midbody is a key regulator of the terminal stages of cell division [16]. Drugs affecting cytokinesis, such as Polo-like kinase-1 (PLK-1) and Aurora kinase inhibitors, have been considered for the treatment of cancers, and new drugs capable of inhibiting cellular division are needed.
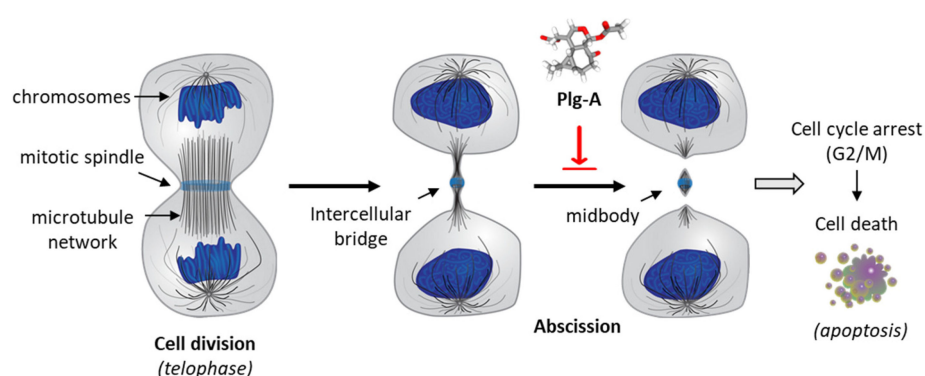
Figure 2. Cytokinesis inhibition by plagiochilin A (Plg-A). At the telophase stage of mitosis, prior to cell division, the two cells are connected by an intercellular bridge with a central midbody. Plg-A prevents completion of cytokinesis at the final abscission stage, blocking cell division (red arrow). The drug-induced inhibition of the late stage of cytokinesis leads to cell cycle arrest (G2/M) and subsequent induction of apoptotic cell death [14].

The molecular target of Plg-A is unknown at present but, based on previous studies, we hypothesized that the natural product could bind to tubulin dimers so as to block the recruitment of α- and β-tubulins for microtubule nucleation. The pironetin-binding site of α-tubulin is known to accommodate compounds bearing a dihydro-pyrone moiety, as found in plagiochilin Q, for example [17,18]. These considerations prompted us to investigate the potential binding of plagiochilins to α-tubulin using molecular modeling. Here, we report a molecular docking analysis of all 24 plagiochilins in relation to the pironetin site of α-tubulin with the objectives of identifying the best potential binders in the series and guiding the development of plagiochilin analogues. The study identified plagiochilin G as the best α-tubulin-interacting compound in the series and provided important structure–binding relationships. Based on these observations, we can propose a rational mechanism of action for a highly potent hemisynthetic plagiochilin derivative discovered in the past [19,20]. The study provides novel perspectives to guide the design of tumor-active plagiochilin derivatives.

2. Materials and Methods

2.1. Molecular Structure and Software

The molecular structure of α-tubulin interacting with pironetin was obtained from the Protein Data Bank (www.rcsb.org (accessed on 9 March 2023)) under the PDB code 5FNV. It corresponds to a high-resolution structure (2.61 Å resolution) of rat α-tubulin expressed in *E. coli* determined by X-ray diffraction [21]. We used the GOLD 5.3 package from the Cambridge Crystallographic Data Centre (Cambridge, UK) to perform the docking experiments with the support of the molecular graphic system provided by Discovery Studio Visualizer, Biovia 2020 (Dassault Systèmes BIOVIA Discovery Studio Visualizer 2020; San Diego, CA, USA, Dassault Systèmes, 2020). For the determination of the potential drug-binding sites on α-tubulin, we used the web server CASTp 3.0 (Computed Atlas of Surface Topography of Proteins) as it is well-suited for the definition of cavities on a protein surface and the specific amino acid positioning, which is important for the interaction. The updated CASTp web server is convenient for studying protein surface architecture and the functional regions with the key residues implicated in the interaction [22,23]. For analysis and visualization, the molecular modeling software Chimera 1.15 was used (https://www.cgl.ucsf.edu/chimera/ (accessed on 9 March 2023)).

2.2. Molecular Modeling Procedure

For model building and evaluation, we used an iterative multi-step procedure. BOSS software (Biochemical and Organic Simulation System, available at http://zarbi.chem.yale.edu/software.html (accessed on 9 March 2023)) was used to perform a Monte Carlo

(MC) conformational search of the different ligands [24]. Within BOSS, a general-purpose molecular mechanics engine capable of performing various calculations, the MS simulation, was realized in the isothermal-isobaric (NPT, constant number of particles, constant pressure and constant temperature) ensemble. The analysis of conformations defines the optimum geometry for each natural product. Thus, the minimum-energy conformers were identified through energy minimization. The next step involved the calculation of the free energy of hydration (ΔG) for a given structure of the compound. Knowledge about the ΔG is useful for investigating the origin of hydrophobic interactions. For this, the molecular mechanics/generalized Born surface area (MM/GBSA) procedure was used according to a described procedure [25]. The MC search and computation of ΔG were performed within BOSS using the xMCGB script according to previously described procedures [25,26].

In our docking procedure, the pironetin-binding site on tubulin was defined as the ligand-binding site for all naturally occurring plagiochilins and derivatives. With the 5FNV structure, the following flexible amino acids were defined during the docking with the GOLD procedure based on shape complementarity criteria: Phe135, Phe202, Leu248, Leu252, Phe255, Gln256, Leu259, Cys316, Lys352 and Leu378. Shape complementarity and geometry considerations favored a docking grid defined from the volume of the central amino acid. In our typical docking process, we used the ChemPLP scoring function to define the 100 best energetically favorable poses and search for the optimized binding mode of the test ligand. Each pose was analyzed and their rankings, aided by the PLP fitness scoring function available from GOLD version 5.3, helped to identify the best trial poses [27]. We usually kept up to six poses per compound and, for the ranked complexes, the empirical potential energy of the interaction ΔE was evaluated using the equation ΔE (interaction) = E (complex) − [E (protein) + E (ligand)]. Energies were calculated on the basis of the Spectroscopic Potential Algorithm for Simulating Biomolecular conformational Adaptability (SPASIBA) spectroscopic force field, a convenient system for the prediction of conformational relative energies derived from vibrational wavenumbers obtained from the infrared and Raman spectra of a large series of compounds, including organic molecules, amino acids, saccharides, nucleic acids and lipids. SPASIBA is essential to define the best protein–ligand structure. It has been specifically developed to provide refined empirical molecular mechanics force field parameters [28–30]. SPASIBA is integrated into the CHARMM force field [31], which was found to be excellent at reproducing crystal-phase infrared data. Overall, this iterative procedure was used to build, analyze and compare the various drug–protein complexes.

3. Results

3.1. Comparative Docking of Plagiochilins to α-Tubulin

The crystal structure of the reference natural product pironetin bound to an α/β-tubulin dimer was used as a template (PDB: 5FNV) to study the binding of plagiochilins to α-tubulin. Each of the 24 compounds was docked into the pironetin site and the most energetically favorable conformation was identified in each case. There was a small binding pocket in the center of the protein, sufficiently deep to completely accommodate a ligand such as plagiochilin A, as represented in Figure 3. The compound was fully engaged in the cavity, inserting its epoxide unit deep into the pocket. All portions of the molecule contributed to the protein interaction, with three notable potential H-bonds with residues Ser241, Gln256 and Lys352, in addition to an array of van der Waals contacts and alkyl/π-alkyl interactions. The epoxide unit of Plg-A interacted with Lys352, whereas the two acetyl groups were engaged in H-bonds with Ser241 and Gln256. Twenty-four similar models were built with the different plagiochilins. A specific model was elaborated for each compound, maintaining the same binding site. The 24 models were then analyzed and compared. For each compound and each model, the empirical energy of interaction (ΔE) and free energy of hydration (ΔG) were calculated (Table 1). Significant variations among the compounds were observed, from −37.9 kcal/mol for the weakest ligand Plg-N to −77.0 kcal/mol for the best compound Plg-G. The free energy of hydration (ΔG) also varied

significantly from one compound to another. Calculated ΔG is a molecular descriptor that usually correlates reasonably well with experimental water solubility.
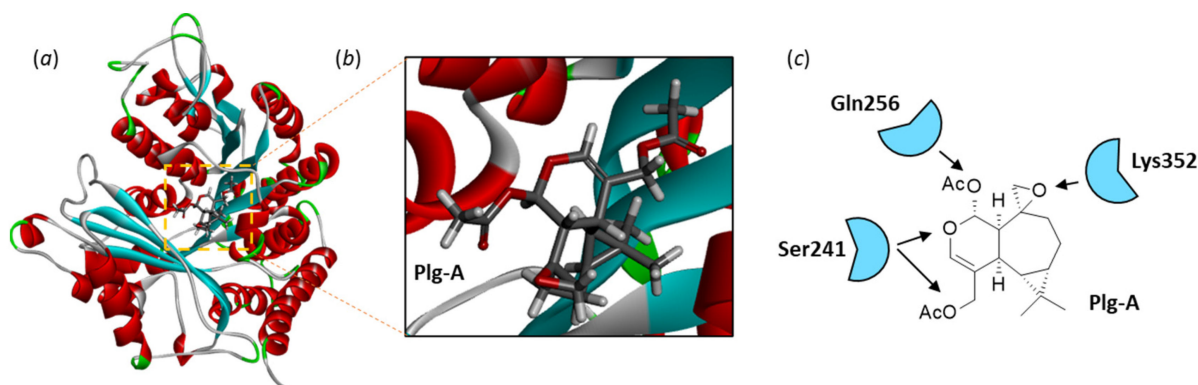

Figure 3. Molecular model of Plg-A bound to α-tubulin (PDB: 5FNV). (**a**) A ribbon model of α-tubulin with bound Plg-A. The α-helices (in red) and β-sheets (in cyan) are shown. (**b**) A close-up view of Plg-A bound to the pironetin site. (**c**) A representation of the main Plg-A/α-tubulin contacts (H-bonds) with the indicated amino acid residues.

Table 1. Potential energy of interaction (ΔE) and free energy of hydration (ΔG) for the interaction between plagiochilins and α-tubulin.

Compounds	ΔE (kcal/mol)	ΔG (kcal/mol)
PlgA-octanoate	−77.50	−28.40
Plagiochilin G	−77.00	−26.00
Plg-OH	−72.40	−22.20
Plagiochilin E	−71.00	−17.20
Plagiochilin D	−67.30	−19.10
Plagiochilin P	−66.85	−24.00
Plagiochilin R	−66.50	−25.50
Plagiochilin O	−64.40	−23.70
Plagiochilin A	−63.80	−19.90
Plagiochilin T	−63.10	−23.30
Plagiochilin B	−62.30	−26.00
Plagiochilin U	−60.40	−20.90
Plagiochilin F	−59.30	−23.15
Plagiochilin L	−57.60	−22.70
Plagiochilin V	−57.45	−16.10
Plagiochilin M	−53.70	−21.20
Plagiochilin S	−53.40	−20.70
Plagiochilin I	−53.25	−16.80
Plagiochilin K	−52.10	−15.50
Plagiochilin C	−47.80	−18.55
Plagiochilin W	−46.60	−19.90
Plagiochilin H	−44.00	−21.30
Plagiochilin J	−42.40	−18.40
Plagiochilin X	−41.30	−20.00
Plagiochilin Q	−39.30	−17.30
Plagiochilin N	−37.90	−15.10
Pironetin	−57.32	−24.20

Plg-A can form stable complexes with α-tubulin characterized by an energy of interaction (ΔE) of −63.8 kcal/mol, more favorable (more negative) than the energy calculated with the reference ligand pironetin. The tubulin-binding capacity was found to vary significantly among the plagiochilins, as represented in Figure 4. Some plagiochilin derivatives, such as Plg-C, -H, -J, -N, -Q, -X and -W, only showed a weak tubulin-binding capacity

(ΔE < 50 kcal/mol). In contrast, the five compounds Plg-D, -O, -P, -R and -T revealed tubulin-binding aptitudes similar or superior to that of Plg-A. A representative model of Plg-D bound to the pironetin site of α-tubulin is shown in Figure 5. This peracetylated compound can form apparently very stable complexes with the tubulin protein stabilized by five H-bonding interactions with residues Ser241, Asn249, Asn258, Cys316 and Lys352, in addition to several weaker van der Waals contacts. The carbonyl groups are major elements in the drug–protein interaction. Plg-D differs from Plg-A in having two addition acetyl groups at positions 12 and 13 of the seco-aromadendrane scaffold, but only the acetyl at position 12 is implicated in the protein interaction. A comparable situation was observed with Plg-P and –R, for which the addition of an -OAc substituent at position 13 led to a significant reinforcement of the tubulin-binding capacity. However, the binding energy calculated with Plg-P was only 5% superior (more negative) to that obtained with Plg-A, a modest improvement. Depending on the products, one of the -OAc substituents—at position 12 or 13—serves as a binding point to stabilize the protein interaction.
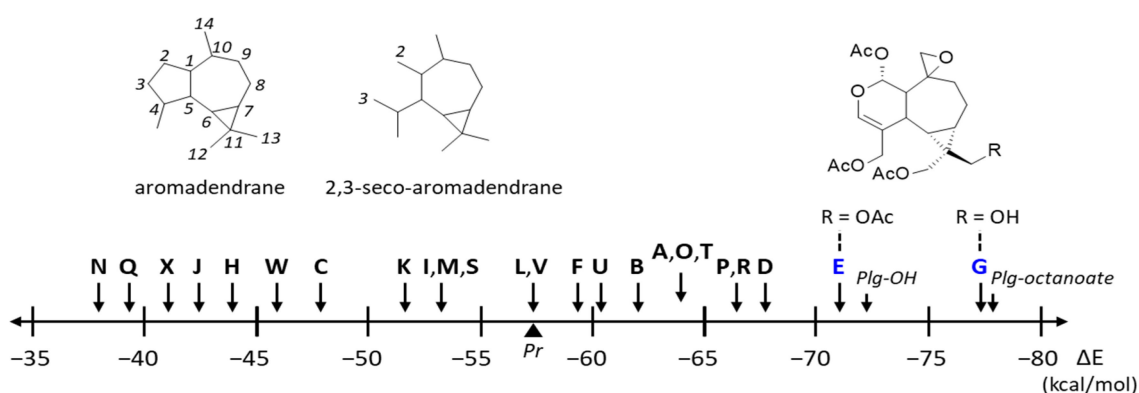

Figure 4. Representation of the empirical energy of interaction (ΔE) calculated with each plagiochilin derivative and the reference compound pironetin (Pr). Values obtained with the derivatives Plg-OH and plagiochilin A-15-yl n-octanoate (plg-octanoate) are also indicated. The top part of the figure shows the structures of the aromadendrane and 2,3-seco-aromadendrane scaffolds (with the numbering scheme) and the structural analogy between the two best compounds Plg-E and G (in blue).
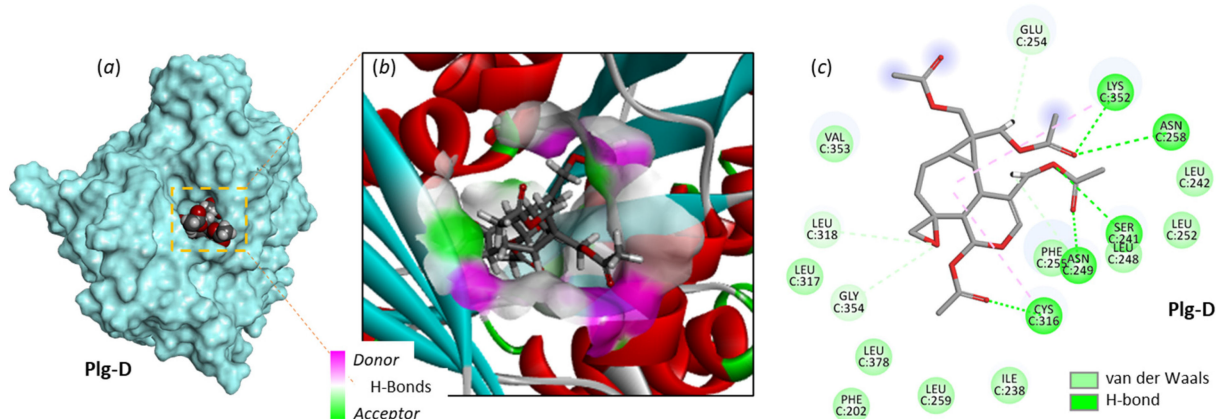

Figure 5. Molecular model of Plg-D bound to α-tubulin. (**a**) A surface model showing that Plg-D fits into a deep central cavity of the protein. (**b**) A detailed view of the Plg-G-binding site with the H-bond donor/acceptor groups surrounding the drug-binding zone (color code indicated). (**c**) Binding map contacts for Plg-D bound to α-tubulin (color code indicated).

Interestingly, two compounds emerged from the docking analysis, Plg-E and –G, with binding capacities significantly superior to that of Plg-A in both cases. The best compound

in the series was Plg-G, with an empirical energy of interaction of −77 kcal/mol, 20% better than that of Plg-A. This compound fit well into the pironetin site, placing its bicyclic core at the bottom of the binding cavity and utilizing the acetyl groups for the protein anchorage. The OH group at C-13 was chiefly implicated in the interaction via two major H-bonds with Ile238 and Ser241 (Figure 6). A similar model was obtained with Plg-E. This point has implications in term of drug design (see below). The epoxide unit of Plg-G also participated in the protein interaction via residue Lys352, as observed with Plg-A. No less than 24 molecular contacts between the compound and α-tubulin were identified in this case, including 4 potential H-bonds and 18 van der Waals contacts, solidly maintaining the stability of the natural product–protein complex. The complex formed with Plg-E was similar, with key H-bonds with Ser241 and Lys352 and an array of van der Waals contacts (not shown). The oxygen atoms of the two OAcetyl groups of Plg-E at C12 and C13 were both involved in the protein interaction. To sum up, the docking analysis supported the hypothesis that plagiochilins can form stable complexes with α-tubulin and suggested that two specific derivatives, plagiochilins E and G, are particularly well-adapted to bind to the pironetin site of α-tubulin.
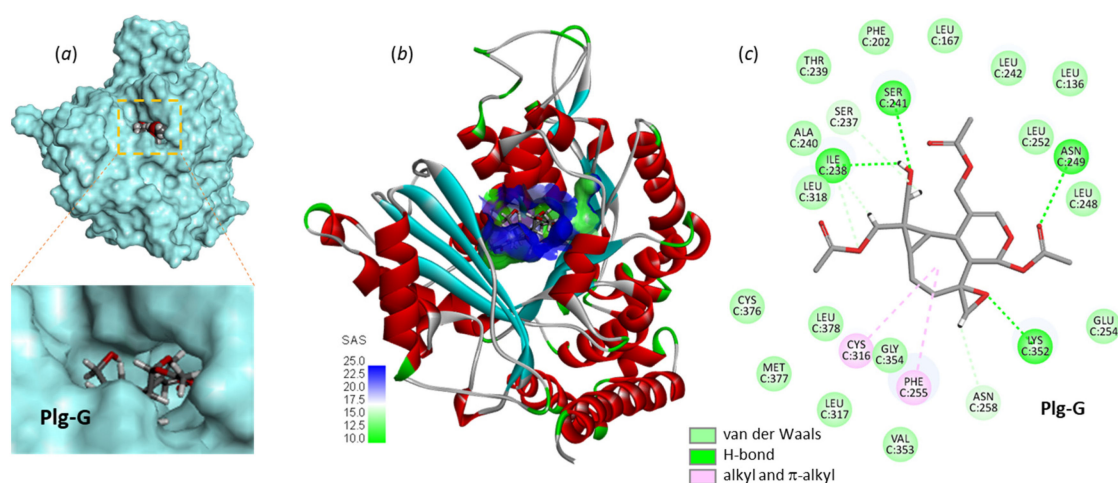

Figure 6. Molecular model of Plg-G bound to α-tubulin. (**a**) Surface model with a close-up view of the binding cavity that accommodates the compound. (**b**) A view of the Plg-G-binding site with the solvent-accessible surface (SAS) surrounding the drug-binding zone (color code indicated). (**c**) Binding map contacts for Plg-G bound to α-tubulin (color code indicated).

3.2. Drug Design Implications

The docking analysis helped us to identify drug substituents of the plagiochilin scaffold important for protein binding. The epoxide moiety of Plg-A together with its two OAc substituents contribute significantly to the protein interaction, as represented in Figure 3c. However, the main discovery is the possibility of significantly reinforcing the interaction when a hydroxyl or acetyl group is introduced at positions C-12 and/or C-13. The optimal configuration was observed with Plg-G bearing a C-13 OH group. Based on this observation, we searched the literature for plagiochilin derivatives possibly bearing such a functional group. We could not directly find such a compound but, interestingly, we identified the derivative plagiochilin A-15-yl n-octanoate (Figure 7), which was presented many years ago as a highly active antiproliferative compound, 60 times more potent against P-388 leukemia cells than the parent compound Plg-A (ID$_{50}$ = 0.05 and 3.0 μg/mL, respectively) [18]. This compound is an ester with an octanoate side chain that may serve as a lipophilic carrier to enhance the bioavailability of the compound. Such ester derivatives are generally unstable in vivo and can hydrolyze to release the corresponding acid (caprylic acid in the present case) and the alcohol derivative, which we designated here as Plg-OH (Figure 7). Therefore, we modeled these two plagiochilin derivatives in interaction with

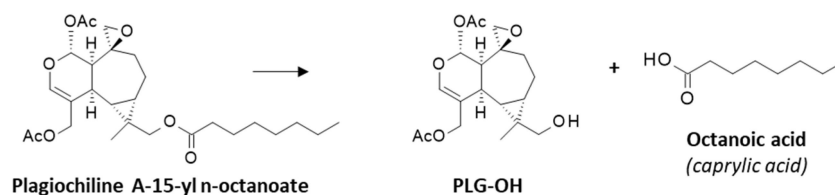α-tubulin to determine the potential contribution of the C13-OH or C=O group to the protein interaction.

Figure 7. Structure of the hemisynthetic derivative plagiochilin A-15-yl n-octanoate and its suspected hydrolysis for the release of the alcohol derivative Plg-OH and the corresponding acid.

The ΔE value calculated with Plg-OH was intermediate between those of Plg-E and Plg-G (Table 1 and Figure 4). The binding configuration could be superimposed well with that of Plg-G, implicating the same H-bonds with residues Ile238, Ser241 and Lys352. The two models were very similar (not shown). Therefore, the alcohol derivative Plg-OH could be used as a starting point to design other esters, ethers or different entities. In addition, surprisingly, we observed that the elongated compound bearing the octanoate side chain could also fit well into the binding cavity. The ΔE value for PlgA-octanoate (−77.5 kcal/mol) was identical to that of Plg-G, the best compound in the series. The presence of the long alkyl chain did not prevent drug binding but contributed to the stability of the drug–protein complex. The model in Figure 8 shows the folding of the compound, placing the alkyl chain into the cavity, in interaction with the protein via van der Walls and alkyl contacts. The interaction of PlgA-octanoate with α-tubulin may contribute, at least partially, to its potent antiproliferative activity.
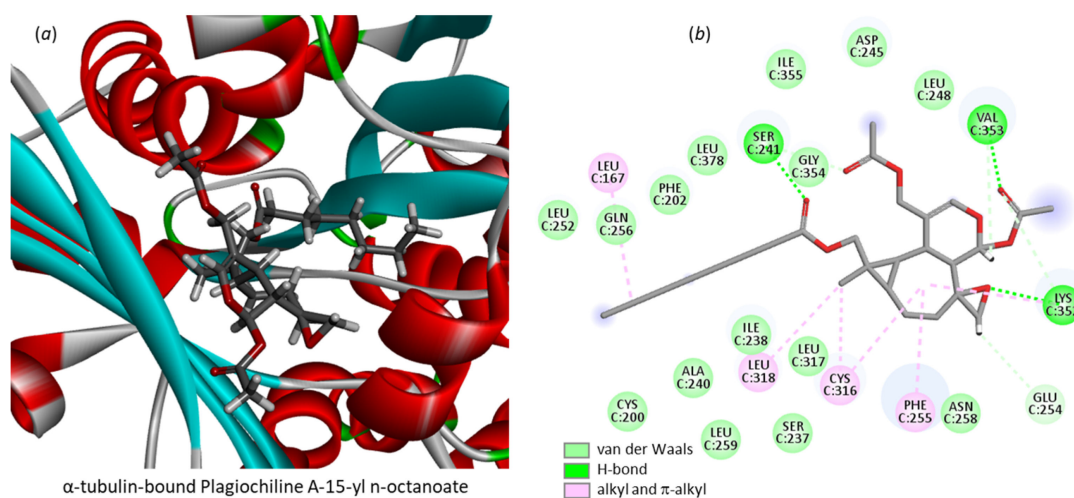

Figure 8. A model of plagiochilin A-15-yl n-octanoate bound to the pironetin site of α-tubulin (**a**) and the corresponding contact map (**b**) with the indicated color code.

4. Discussion

Bryophytes (non-vascular plants) are extremely abundant and diversified. The group includes three main subcategories: Bryophyta (mosses), Marchantiophyta (liverworts) and Anthocerotophyta (hornworts). More than 7400 species of liverworts and hornworts have been inventoried [32]. The genus *Plagiochila* refers to one of the most important groups of leafy liverworts, with >500 species distributed across all continents and territories [33]. However, Plagiochilaceae have been little studied thus far. They represent a potential source of bioactive compounds, such as the plagiochilins studied here, as well as sesquiterpenoids (plagicosins) and alkaloids (plagiochianins), as discussed recently [7].

The series of plagiochilins has been characterized over the past 30 years, mainly from a natural product discovery perspective. The 24 derivatives have been successively isolated

and structurally identified, but their biological and pharmacological properties have not been significantly investigated. Antiparasitic and anticancer effects have been reported, essentially for Plg-A and Plg-C [10,19,34–37]. The other compounds are somewhat neglected at present. However, a major study recently provided a key element to understand the mechanism of action of the lead product Plg-A. The product was identified as a potent inhibitor of cytokinesis and its antimitotic effects are likely at the origin of the antiproliferative action of the compound [14]. Plg-A was shown to induce specific mitotic figures, with accumulation of dividing DU145 cells connected with intercellular bridges, corresponding to the abscission stage of cytokinesis. By so doing, the natural product reduced the number and size of DU145 cell colonies and induced cell death [14]. Plg-A exerts an effect on the cytoskeleton, with a rearrangement of α-tubulin characteristic of cytokinetic membrane abscission. Based on these observations, we postulated that the compound could alter the microtubule-organizing center that recruits α- and β-tubulins for microtubule nucleation. We postulated that the compound could bind the pironetin-binding site of α-tubulin, which is known to accommodate compounds bearing a dihydro-pyrone moiety [17,18]. This moiety can be found in plagiochilin Q, and we recently showed that a related series of natural products with a 5,6-dihydro-α-pyrone unit, the cryptoconcatones, can function as α-tubulin-binding agents. Notably, we identified cryptoconcatones F and L as robust α-tubulin binders capable of forming covalent protein adducts [38]. We also found evidence of the cytotoxic lactone spicigerolide with a pyranone moiety as a tubulin binder. These considerations prompted us to investigate the binding of plagiochilins to α-tubulin.

The molecular modeling analysis suggests that several plagiochilin derivatives can form stable complexes with α-tubulin via binding to the pironetin site. The best potential binders are Plg-E and Plg-G, which are structurally similar. The analysis points to the key role of the C13-OH or O-C=O group in the interaction with tubulin. The importance of this unit was further investigated with the two compounds Plg-OH and plagiochilin A-15-yl n-octanoate, both identified as potent α-tubulin-binding agents. The observation is important to guide future drug design in the series. Analogues bearing different ester groups or other side chains could be designed. The study opens novel perspectives for the discovery and design of novel plagiochilin-like molecules. The difficulty is obtaining the starting materials for synthesis. Thus far, only the total (and difficult—16 steps) synthesis of Plg-N has been reported, starting from the anthelmintic sesquiterpene lactone santonin [39]. However, options exist to obtain sufficient quantities of Plg-A to perform hemisyntheses. *Plagiochila* biomass can be produced under laboratory conditions through bryo-reactors and molecular farming [40]. Through such biotechnological processes, secondary metabolites from bryophytes can be produced in large quantities, allowing the exploitation of their pharmaceutical properties. A new era of bryo-pharmaceuticals is put into perspective [41]. Bryophytes are increasingly considered as a source of medicinal products, notably as antifungal agents [3].

Without doubt, *Plagiochila* species warrant further investigations as a source of bioactive compounds. Different molecules of biopharmaceutical interest have been isolated recently from various species, such as *P. porelloides*, which has enabled the development of novel antiparasitic compounds [42]. A series of terpenoids designated plagicosins A–N, isolated from the Chinese liverwort *P. fruticosa* Mitt., have been characterized, with the lead compound plagicosin F inhibiting the adhesion and biofilm formation of the fungus *Candida albicans* [43]. There are also interesting macrocyclic bisbibenzyl compounds, such as isoplagiochins C and D from *P. fruticosa* and other species [44,45]. Plagiochilins—notably, the lead molecules plagiochilin A and plagiochilin G—are emerging as an interesting series of anticancer agents. Plg-G was isolated more than 40 years ago from *P. ovalifolia* Mitt. [34], the same species that produced Plg-N [39], and plagiochilin A-15-yl octanoate [19]. *P. ovalifolia* is an eastern Asiatic species, so far known essentially from China, Japan, the Republic of Korea and the Philippines [46]. It is possible to establish suspension cultures from callus tissue induced by culturing spores of *P. ovalifolia* [47]. Therefore, there is a possibility of generating plagiochilin derivatives. Hopefully, our docking analysis will promote research

on *Plagiochila* and plagiochilins. Beyond the plagiochilins, this work reinforces the interest of targeting *α*-tubulin and the pironetin site, still considered an underexplored target for cancer therapeutics [18]. The present study adds a few new compounds to the list of natural products with microtubule-destabilizing properties. The design of novel plagiochilin A derivatives should be highly encouraged.

Our work suggests a direct interaction between Plg-A and some derivatives and *α*-tubulin, but tubulin may not be the unique molecular target. The compounds may well bind to other proteins implicated in microtubule dynamics, or they may not. For example, the binding of Plg-A to the pteridine reductase 1 of the parasite *Leishmania major* has been proposed based on a docking study [48]. Binding to different proteins cannot be excluded, but priority should be given to the study of Plg-A-induced interference with microtubules and microtubule-associated proteins.

Author Contributions: G.V.: Visualization; Software; Computations; Molecular modeling. C.B.: Conceptualization; Investigation; Visualization; Writing—original draft; Writing—review and editing. All authors have read and agreed to the published version of the manuscript.

Institutional Review Board Statement: Not applicable.

Informed Consent Statement: Not applicable.

Data Availability Statement: Data sharing not applicable.

Conflicts of Interest: The authors declare no conflict of interest.

References

1. Frangedakis, E.; Shimamura, M.; Villarreal, J.C.; Li, F.W.; Tomaselli, M.; Waller, M.; Sakakibara, K.; Renzaglia, K.S.; Szövényi, P. The hornworts: Morphology, evolution and development. *New Phytol.* **2021**, *229*, 735–754. [CrossRef] [PubMed]
2. Drobnik, J.; Stebel, A. Four Centuries of Medicinal Mosses and Liverworts in European Ethnopharmacy and Scientific Pharmacy: A Review. *Plants* **2021**, *10*, 1296. [CrossRef] [PubMed]
3. Commisso, M.; Guarino, F.; Marchi, L.; Muto, A.; Piro, A.; Degola, F. Bryo-Activities: A Review on How Bryophytes Are Contributing to the Arsenal of Natural Bioactive Compounds against Fungi. *Plants* **2021**, *10*, 203. [CrossRef] [PubMed]
4. Asakawa, Y.; Nagashima, F.; Ludwiczuk, A. Distribution of Bibenzyls, Prenyl Bibenzyls, Bis-bibenzyls, and Terpenoids in the Liverwort Genus Radula. *J. Nat. Prod.* **2020**, *83*, 756–769. [CrossRef]
5. Ludwiczuk, A.; Asakawa, Y. Bryophytes as a source of bioactive volatile terpenoids—A review. *Food Chem. Toxicol.* **2019**, *132*, 110649. [CrossRef]
6. Asakawa, Y.; Toyota, M.; Takemoto, T. Plagiochilide et plagiochiline a, secoaromadendrane-type sesquiterpenes de la mousse, *plagiochila yokogurensis* (plagiochilaceae). *Tetrahedron Lett.* **1978**, *19*, 1553–1556. [CrossRef]
7. Asakawa, Y.; Toyota, M.; Takemoto, T. La plagiochiline a et la plagiochiline b, les sesquiterpenes du type secoaromadendrane de la mousse, *Plagiochila hattoriana*. *Phytochemistry* **1978**, *17*, 1794. [CrossRef]
8. Asakawa, Y.; Toyota, M.; Takemoto, T.; Suire, C. Plagiochilines C, D, E and F, four novel secoaromadendrane-type sesquiterpene hemiacetals from *Plagiochila asplenioides* and *Plagiochila semidecurrens*. *Phytochemistry* **1979**, *18*, 1355–1357. [CrossRef]
9. Fukuyama, Y.; Toyota, M.; Asakawa, Y. Ent-kaurene diterpene from the liverwort *Plagiochila pulcherrima*. *Phytochemistry* **1988**, *27*, 1425–1427. [CrossRef]
10. Aponte, J.C.; Yang, H.; Vaisberg, A.J.; Castillo, D.; Málaga, E.; Verástegui, M.; Casson, L.K.; Stivers, N.; Bates, P.J.; Rojas, R.; et al. Cytotoxic and anti-infective sesquiterpenes present in *Plagiochila disticha* (Plagiochilaceae) and *Ambrosia peruviana* (Asteraceae). *Planta Med.* **2010**, *76*, 705–707. [CrossRef]
11. Asakawa, Y.; Inoue, H.; Toyota, M.; Takemoto, T. Sesquiterpenoids of fourteen *Plagiochila* species. *Phytochemistry* **1980**, *19*, 623–2626. [CrossRef]
12. Bailly, C. Discovery and anticancer activity of the *plagiochilins from the* liverwort genus Plagiochila. *Life* **2023**, *13*, 758. [CrossRef]
13. Asakawa, Y. Chemosystematics of the hepaticae. *Phytochemistry* **2004**, *65*, 623–669. [CrossRef]
14. Stivers, N.S.; Islam, A.; Reyes-Reyes, E.M.; Casson, L.K.; Aponte, J.C.; Vaisberg, A.J.; Hammond, G.B.; Bates, P.J. Plagiochiline A Inhibits Cytokinetic Abscission and Induces Cell Death. *Molecules* **2018**, *23*, 1418. [CrossRef]
15. McNeely, K.C.; Dwyer, N.D. Cytokinetic Abscission Regulation in Neural Stem Cells and Tissue Development. *Curr. Stem Cell Rep.* **2021**, *7*, 161–173. [CrossRef]

16. Peterman, E.; Prekeris, R. The postmitotic midbody: Regulating polarity, stemness, and proliferation. *J. Cell. Biol.* **2019**, *218*, 3903–3911. [CrossRef]

17. Huang, D.S.; Wong, H.L.; Georg, G.I. Synthesis and Cytotoxicity Evaluation of C4- and C5-Modified Analogues of the α,β-Unsaturated Lactone of Pironetin. *ChemMedChem* **2017**, *12*, 520–528. [CrossRef]

18. Coulup, S.K.; Georg, G.I. Revisiting microtubule targeting agents: α-Tubulin and the pironetin binding site as unexplored targets for cancer therapeutics. *Bioorg. Med. Chem. Lett.* **2019**, *29*, 1865–1873. [CrossRef]

19. Toyota, M.; Tanimura, K.; Asakawa, Y. Cytotoxic 2,3-secoaromadendrane-type sesquiterpenoids from the liverwort *Plagiochila ovalifolia*. *Planta Med.* **1998**, *64*, 462–464. [CrossRef]

20. Toyota, M.; Nakamura, I.; Huneck, S.; Asakawa, Y. Sesquiterpene esters from the liverwort *Plagiochila porelloides*. *Phytochemistry* **1994**, *37*, 1091–1093. [CrossRef]

21. Yang, J.; Wang, Y.; Wang, T.; Jiang, J.; Botting, C.H.; Liu, H.; Chen, Q.; Yang, J.; Naismith, J.H.; Zhu, X.; et al. Pironetin reacts covalently with cysteine-316 of α-tubulin to destabilize microtubule. *Nat. Commun.* **2016**, *7*, 12103. [CrossRef] [PubMed]

22. Dundas, J.; Ouyang, Z.; Tseng, J.; Binkowski, A.; Turpaz, Y.; Liang, J. CASTp: Computed atlas of surface topography of proteins with structural and topographical mapping of functionally annotated residues. *Nucleic Acids Res.* **2006**, *34*, W116–W118. [CrossRef] [PubMed]

23. Tian, W.; Chen, C.; Lei, X.; Zhao, J.; Liang, J. CASTp 3.0: Computed atlas of surface topography of proteins. *Nucleic Acids Res.* **2018**, *46*, W363–W367. [CrossRef] [PubMed]

24. Jorgensen, W.L.; Tirado-Rives, J. Monte Carlo versus Molecular Dynamics for conformational sampling. *J. Phys. Chem.* **1996**, *100*, 14508–14513. [CrossRef]

25. Jorgensen, W.L.; Tirado-Rives, J. Molecular modeling of organic and biomolecular systems using BOSS and MCPRO. *J. Comput. Chem.* **2005**, *26*, 1689–1700. [CrossRef]

26. Jorgensen, W.L.; Ulmschneider, J.P.; Tirado-Rives, J. Free energies of hydration from a generalized Born model and an ALL-atom force field. *J. Phys. Chem. B* **2004**, *108*, 16264–16270. [CrossRef]

27. Jones, G.; Willett, P.; Glen, R.C.; Leach, A.R.; Taylor, R. Development and validation of a genetic algorithm for flexible docking. *J. Mol. Biol.* **1997**, *267*, 727–748. [CrossRef]

28. Meziane-Tani, M.; Lagant, P.; Semmoud, A.; Vergoten, G. The SPASIBA force field for chondroitin sulfate: Vibrational analysis of D-glucuronic and N-acetyl-D-galactosamine 4-sulfate sodium salts. *J. Phys. Chem. A* **2006**, *110*, 11359–11370. [CrossRef]

29. Vergoten, G.; Mazur, I.; Lagant, P.; Michalski, J.C.; Zanetta, J.P. The SPASIBA force field as an essential tool for studying the structure and dynamics of saccharides. *Biochimie* **2003**, *85*, 65–73. [CrossRef]

30. Lagant, P.; Nolde, D.; Stote, R.; Vergoten, G.; Karplus, M. Increasing Normal Modes Analysis Accuracy: The SPASIBA Spectroscopic Force Field Introduced into the CHARMM Program. *J. Phys. Chem. A* **2004**, *108*, 4019–4029. [CrossRef]

31. Homans, S.W. A molecular mechanical force field for the conformational analysis of oligosaccharides: Comparison of theoretical and crystal structures of Man alpha 1-3Man beta 1-4GlcNAc. *Biochemistry* **1990**, *29*, 9110–9118. [CrossRef]

32. Söderström, L.; Hagborg, A.; von Konrat, M.; Bartholomew-Began, S.; Bell, D.; Briscoe, L.; Brown, E.; Cargill, D.C.; da Costa, D.P.; Crandall-Stotler, B.J.; et al. World checklist of hornworts and liverworts. *PhytoKeys* **2016**, *59*, 1–828. [CrossRef]

33. Heinrichs, J.; Hentschel, J.; Feldberg, K.; Bombosch, A.; Schneider, H. Phylogenetic biogeography and taxonomy of disjunctly distributed bryophytes. *J. Syst. Evol.* **2009**, *47*, 497–508. [CrossRef]

34. Asakawa, Y.; Toyota, M.; Takemoto, T. Three *ent*-secoaromadendrane-type sesquiterpene hemiacetals and a bicyclogermacrene from *Plagiochila ovalifolia* and *Plagiochila yokogurensis*. *Phytochemistry* **1980**, *19*, 2141–2145. [CrossRef]

35. Asakawa, Y.; Toyota, M.; Takemoto, T.; Kubo, I.; Nakanishi, K. Insect antifeedant secoaromadendrane-type sesquiterpenes from *Plagiochila* species. *Phytochemistry* **1980**, *19*, 2147–2154. [CrossRef]

36. Asakawa, Y.; Ludwiczuk, A.; Nagashima, F. Phytochemical and biological studies of bryophytes. *Phytochemistry* **2013**, *91*, 52–80. [CrossRef]

37. Wang, S.; Liu, S.S.; Lin, Z.M.; Li, R.J.; Wang, X.N.; Zhou, J.C.; Lou, H.X. Terpenoids from the Chinese liverwort *Plagiochila pulcherrima* and their cytotoxic effects. *J. Asian Nat. Prod. Res.* **2013**, *15*, 473–481. [CrossRef]

38. Vergoten, G.; Bailly, C. Molecular Docking of Cryptoconcatones to α-Tubulin and Related Pironetin Analogues. *Plants* **2023**, *12*, 296. [CrossRef]

39. Blay, G.; Cardona, L.; García, B.; Lahoz, L.; Pedro, J.R. Synthesis of plagiochilin N from santonin. *J. Org. Chem.* **2001**, *66*, 7700–7705. [CrossRef]

40. Sabovljević, M.S.; Ćosić, M.V.; Jadranin, B.Z.; Pantović, J.P.; Giba, Z.S.; Vujičić, M.M.; Sabovljević, A.D. The Conservation Physiology of Bryophytes. *Plants* **2022**, *11*, 1282. [CrossRef]

41. Pandey, S.; Alam, A. Bryo-Pharmaceuticals: An Emerging Era of Pharmaceutical Products. In *Advanced Pharmacological Uses of Medicinal Plants and Natural Products*; IGI Global: Hershey, PA, USA, 2020; Chapter 14; pp. 269–284. [CrossRef]

42. Pannequin, A.; Quetin-Leclercq, J.; Costa, J.; Tintaru, A.; Muselli, A. First Phytochemical Profiling and *In-Vitro* Antiprotozoal Activity of Essential Oil and Extract of *Plagiochila porelloides*. *Molecules* **2023**, *28*, 616. [CrossRef] [PubMed]

43. Qiao, Y.N.; Jin, X.Y.; Zhou, J.C.; Zhang, J.Z.; Chang, W.Q.; Li, Y.; Chen, W.; Ren, Z.J.; Zhang, C.Y.; Yuan, S.Z.; et al. Terpenoids from the Liverwort *Plagiochila fruticosa* and Their Antivirulence Activity against *Candida albicans*. *J. Nat. Prod.* **2020**, *83*, 1766–1777. [CrossRef] [PubMed]

44. Nagashima, F.; Sekiguchi, T.; Takaoka, S.; Asakawa, Y. Terpenoids and aromatic compounds from the New Zealand liverworts Plagiochila, Schistochila, and Heteroscyphus species. *Chem. Pharm. Bull.* **2004**, *52*, 556–560. [CrossRef] [PubMed]

45. Bringmann, G.; Mühlbacher, J.; Reichert, M.; Dreyer, M.; Kolz, J.; Speicher, A. Stereochemistry of isoplagiochin C, a macrocyclic bisbibenzyl from liverworts. *J. Am. Chem. Soc.* **2004**, *126*, 9283–9290. [CrossRef]

46. So, M.L.; Grolle, R. Studies on *Plagiochila* sect. *Plagiochila* (Hepaticae) in East and South Asia. *J. Bryol.* **2000**, *22*, 17–28. [CrossRef]

47. Matsuo, A.; Ono, K.; Hamasaki, K.; Nozaki, H. Phaeophytins from a cell suspension culture of the liverwort *Plagiochila ovalifolia*. *Phytochemistry* **1996**, *42*, 427–430. [CrossRef]

48. Ogungbe, I.V.; Setzer, W.N. In-silico Leishmania target selectivity of antiparasitic terpenoids. *Molecules* **2013**, *18*, 7761–7847. [CrossRef]